

UCID- 20533

CIRCULATION COPY
SUBJECT TO RECALL
IN TWO WEEKS

MODELING ON-RESISTANCE FOR SILICON
PHOTOCONDUCTIVE SWITCHING DEVICES

J. D. Morse

August 22, 1985

Lawrence
Livermore
National
Laboratory

This is an informal report intended primarily for internal or limited external distribution. The opinions and conclusions stated are those of the author and may or may not be those of the Laboratory.

Work performed under the auspices of the U.S. Department of Energy by the Lawrence Livermore National Laboratory under Contract W-7405-Eng-48.

DISCLAIMER

This document was prepared as an account of work sponsored by an agency of the United States Government. Neither the United States Government nor the University of California nor any of their employees, makes any warranty, express or implied, or assumes any legal liability or responsibility for the accuracy, completeness, or usefulness of any information, apparatus, product, or process disclosed, or represents that its use would not infringe privately owned rights. Reference herein to any specific commercial products, process, or service by trade name, trademark, manufacturer, or otherwise, does not necessarily constitute or imply its endorsement, recommendation, or favoring by the United States Government or the University of California. The views and opinions of authors expressed herein do not necessarily state or reflect those of the United States Government or the University of California, and shall not be used for advertising or product endorsement purposes.

Printed in the United States of America
Available from
National Technical Information Service
U.S. Department of Commerce
5285 Port Royal Road
Springfield, VA 22161
Price: Printed Copy \$ Microfiche \$4.50

<u>Page Range</u>	<u>Domestic Price</u>	<u>Page Range</u>	<u>Domestic Price</u>
001-025	\$ 7.00	326-350	\$ 26.50
026-050	8.50	351-375	28.00
051-075	10.00	376-400	29.50
076-100	11.50	401-426	31.00
101-125	13.00	427-450	32.50
126-150	14.50	451-475	34.00
151-175	16.00	476-500	35.50
176-200	17.50	501-525	37.00
201-225	19.00	526-550	38.50
226-250	20.50	551-575	40.00
251-275	22.00	576-600	41.50
276-300	23.50	601-up ¹	
301-325	25.00		

¹Add 1.50 for each additional 25 page increment, or portion thereof from 601 pages up.

TABLE OF CONTENTS

	<u>Page</u>
Introduction.....	1
Effects of Electric Field and Carrier-Carrier Interactions.....	4
Temperature Effects.....	5
Conclusion.....	7
References.....	8

LIST OF FIGURES

	<u>Page</u>
Figure 1 - Silicon photoconductive switching device structure.....	9
Figure 2 - Electron (μ_n), hole (μ_p), and ambipolar (μ_a) mobilities as a function of a carrier concentration.....	10
Figure 3 - Switch conductance as a function of absorbed energy assuming a carrier concentration dependent mobility.....	11
Figure 4 - Equivalent circuit of photoconductive switch mounted on 50 ohm transmission lines.....	12
Figure 5 - Switch conductance as a function of absorbed energy assuming field dependent mobility	13
Figure 6 - Comparison of switch conductance as a function of absorbed energy for constant mobility and electric field, carrier concentration dependent mobility.....	14
Figure 7a - Ohmic mobility of electrons in silicon as a function of temperature. It can be seen that for $T \leq 100^\circ\text{K}$, the electron mobility has a $T^{-2.55}$ dependence on temperature....	15
Figure 7b - Ohmic mobility of holes in silicon as a function of temperature. The solid line shows a $T^{-2.2}$ dependence of hole mobility on temperature.....	15
Figure 8 - Switch conductance as a function of absorbed energy at $T=77, 100, 200$ and 300°K	16
Figure 9 - Switch conductance as a function of absorbed energy for $\mu_n \propto T^{-2.42}$ compared to $\mu_n \propto T^{-2.55}$	17

MODELING ON-RESISTANCE FOR SILICON
PHOTOCONDUCTIVE SWITCHING DEVICES

Jeffrey Morse

1. INTRODUCTION

Analytical models have been developed in order to characterize the on-resistance of silicon photoconductive switching devices as a function of the optical energy absorbed. Previously, the switch resistance has been expressed as [1]:

$$R_{on} = \frac{h\nu L V}{q v_d E_a} \quad (1)$$

where $h\nu$ is the energy per photon of incident light, L is the gap length between electrodes, V is the applied voltage, E_a is the absorbed energy and v_d is the carrier drift velocity. From Eq. (1), it can be seen that if v_d were a constant, R_{on} would be directly proportional to the applied voltage.

However, the carrier drift velocity is generally a function of applied voltage. As the energy incident upon the photoconductive switch increases, more carriers are generated, increasing the conductivity, resulting in a decrease in the voltage drop across the switch. At high absorbed energy, there is only a small voltage drop across the device. Therefore, the electric field is reduced in the silicon and the carrier velocity is given by

$$v_d = \mu E_{sw} = \mu V/L \quad (\text{cm/sec}) \quad (2)$$

This work was performed under the auspices of the U.S. Department of Energy by Lawrence Livermore National Laboratory under contract No. W-7405-Eng-48.

From (2), μ is the carrier mobility and E_{sw} is the electric field across the switch.

The photoconductive switching device structure is shown in Fig. 1. For this simple structure, the switch resistance when conducting is described by

$$R = \rho L/A \quad (3)$$

where ρ is the resistivity and A is the cross sectional area of the device.

The resistivity is given by

$$\rho = q(\mu_n n + \mu_p p)^{-1} \quad (4)$$

where the electron and hole concentrations are determined by

$$n = n_0 + n' \quad (5a)$$

$$p = p_0 + p' \quad (5b)$$

where n_0 and p_0 are the equilibrium concentrations, and $n' = p'$ is the excess carrier concentration. For high absorbed energy, $n' \gg n_0$, $p' \gg p_0$.

Substitution of (5a,b) and (4) into (3) gives

$$R = \frac{L}{q(\mu_n + \mu_p)n'A} = \frac{L}{q\mu n'A} \quad (6)$$

From Eq. (6), $\mu = (\mu_n + \mu_p) \approx \mu_n$ for silicon assuming constant mobility. In order to determine the excess carrier concentration generated from the absorbed light, the following two assumptions are made:

- 1) One EHP is generated for each photon absorbed.
- 2) The device thickness is small compared to the absorption length.

Now, the excess carrier concentration can be calculated by

$$\begin{aligned} n' &= \frac{E_a}{h\nu} / \text{Volume} \\ &= \frac{E_a}{h\nu LA} \end{aligned} \quad (7)$$

Combining (6) and (7) gives the expression for the on-resistance as

$$R = \frac{h\nu L^2}{q\mu E_i (1-R)} \quad (8)$$

where $E_a = E_i(1-R)$. E_i is the incident energy and R is the reflectivity of the semiconductor material. The $1/R_{on}$ vs. E_a relation is independent of applied voltage and has a constant slope of

$$\frac{d(1/R_{on})}{dE_a} = 1.92 \times 10^4 \quad (9)$$

for IR light ($\lambda = 1.05 \mu\text{m}$) with a gap length of $L = 2.5 \text{ mm}$. Note that the switch resistance, as given by Eq. (8), is independent of the device thickness and width.

2. EFFECTS OF ELECTRIC FIELD AND CARRIER-CARRIER INTERACTIONS

As the absorbed energy increases, the density of free carriers generated increases. When the excess carrier concentration exceeds $n' > 10^{16} \text{ cm}^{-3}$, the mobility is severely degraded (Fig. 2) [4] due to carrier-carrier interactions. A carrier concentration dependent mobility model

$$\mu(n) = \mu_0 / (C_1 n + C_2) \quad (10)$$

where μ_0 is the mobility at equilibrium, C_1 and C_2 are empirically determined from Fig. 2, replaces the constant mobility in Eq. (8). The curves A and C in Fig. 3 illustrate the switch conductance, absorbed energy relation using this model. For excess carrier concentrations $n' = p' > 10^{17} \text{ cm}^{-3}$, the electron and hole mobilities are comparable. By including the hole mobility in (8), the switch conductance increases by a factor of two. This is illustrated by the curves B and D of Fig. 3. Thus, an ambipolar mobility model is required at higher incident energy. Note that by including the carrier concentration dependent mobility in Eq. (8), the on-resistance becomes a function of the device width and thickness because n = number of carriers generated/volume of device (cm^{-3}), is now implemented in Eq. (10).

At low absorbed energy, the switch resistance will be large, resulting in a large voltage drop across the switch. There is now a substantial electric field within the active area of the switch. A field dependent (Scharfetter-Gummel) [2] mobility model, given by

$$\mu(E) = \mu_0 / \left[1 + \frac{N}{N/S+N_r} + \frac{(E/A)^2}{E/A+F} + (E/B)^2 \right]^{1/2} \quad (11)$$

where E is the electric field, N is the impurity concentration and A, B, F, S, and N_r are empirical constants given by [2] is used in Eq. (8) to calculate the switch on-resistance. Assuming the photoconductive device is mounted on 50 ohm transmission lines, the circuit shown in Fig. 4, along with Eq. (8) are simultaneously solved using iterative techniques in order to determine the voltage across the switch for a given energy absorbed. Figure 5 illustrates the switch conductance vs. E_a for IR light incident at various voltages. Figure 5 assumes a field dependent mobility only. The effects of the electric field on switch conductance are most predominant at lower absorbed energy. As E_a increases, the curves converge.

Next, a full field and carrier concentration dependent mobility model was implemented in Eq. (8). The switch conductance vs. absorbed energy is shown in Fig. 6. It can be seen that for $E_a = 100 \mu J$, a switch resistance of $R_{on} = 3.0$ ohms can be expected. In order to obtain on-resistances less than 1 ohm, energy on the order of a millijoule will be necessary.

3. TEMPERATURE EFFECTS

The effects of reducing the temperature substantially below room temperature significantly improve the characteristics of photoconductive switching devices as follows:

- 1) The absorption coefficient of the semiconductor material will vary with temperature, thus increasing the sensitivity of the device to the incident light.

- 2) The carrier mobility varies with temperature, thereby changing the conductivity of the device.

Only the variations in mobility with decreasing temperature will be considered at this time. The mobility for electrons and holes as a function of temperature is illustrated in Fig. 7a,b, respectively. From Fig. 7, the mobility temperature relationship is determined to be [3]:

$$\mu_n(T) = A_n T^{-2.42} \quad (12)$$

$$\mu_p(T) = A_p T^{-2.2} \quad (13)$$

where A_n and A_p are given by [3]. The conductance vs. absorbed energy is shown in Fig. 8 at various temperatures using the relationships of (12) and (13). The model also uses the carrier concentration and electric field dependent mobility models previously mentioned. It can be seen from Fig. 8 that there is a significant increase in the switch conductance at $T = 77^\circ\text{K}$ over that at room temperature.

By observing the experimental data of Fig. 7a, it can be seen that the relation given by Eq. (12) is only valid over the temperature range $200^\circ\text{K} < T < 1000^\circ\text{K}$. For temperatures below 200°K , a new relation is required to accurately describe the electron mobility as a function of temperature. This relationship can be expressed as

$$\mu_n(T) = A_n T^{-2.55} \quad (14)$$

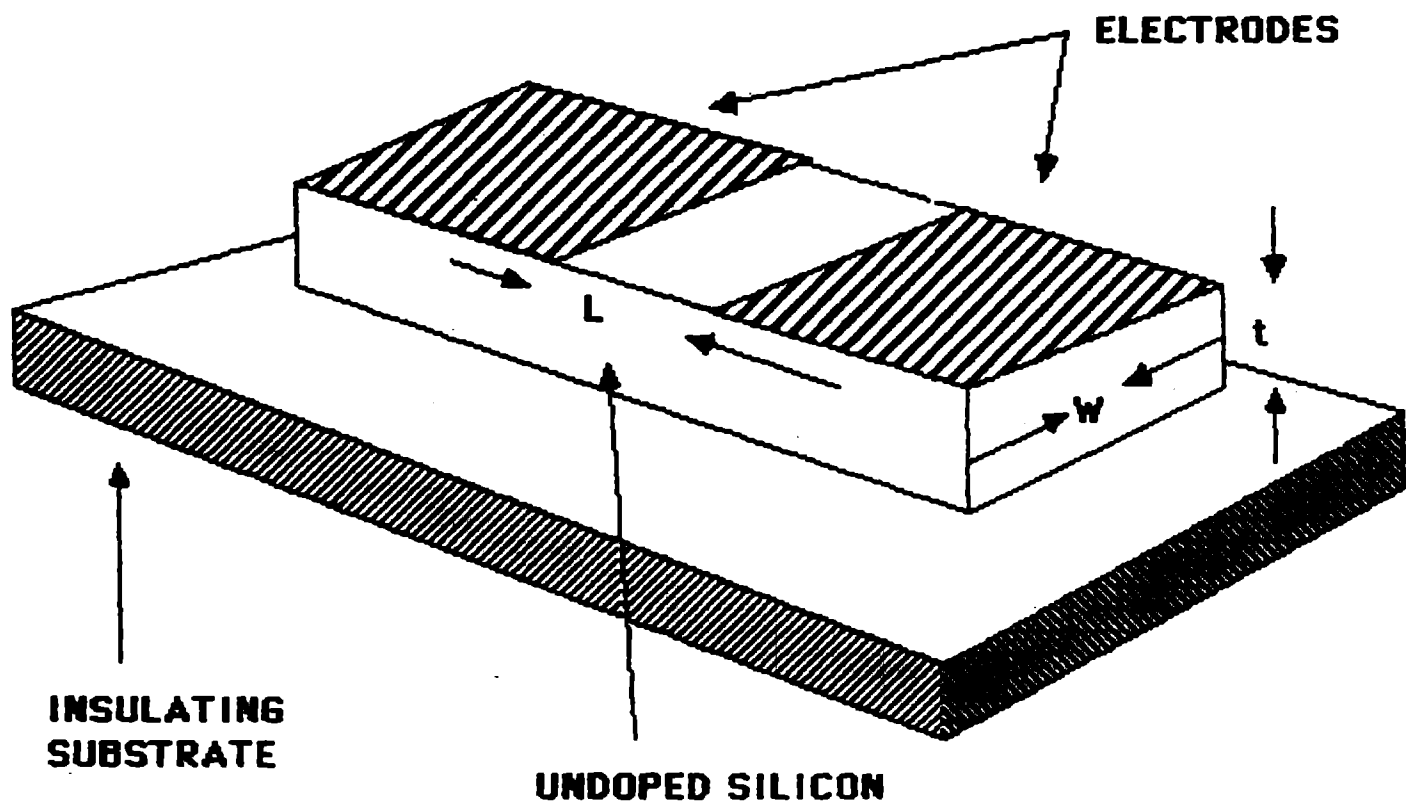
where A_n is the same as in (12). Figure 9 compares the results obtained by using Eq. (14) to those obtained by using Eq. (12) for $T = 77^\circ\text{K}$ and $T = 100^\circ\text{K}$.

4. CONCLUSION

It has been shown that by using a more exact mobility model which accounts for physical effects on the carrier mobility, significant changes in conductance are found for the same device structure. The effects accounted for in this more exact model are electric field degradation, carrier-carrier interactions, and temperature effects. Further work in this area should concentrate on obtaining experimental data to verify these results, along with the development of more exact numerical models to account for two-dimensional drift and diffusion effects on device performance.

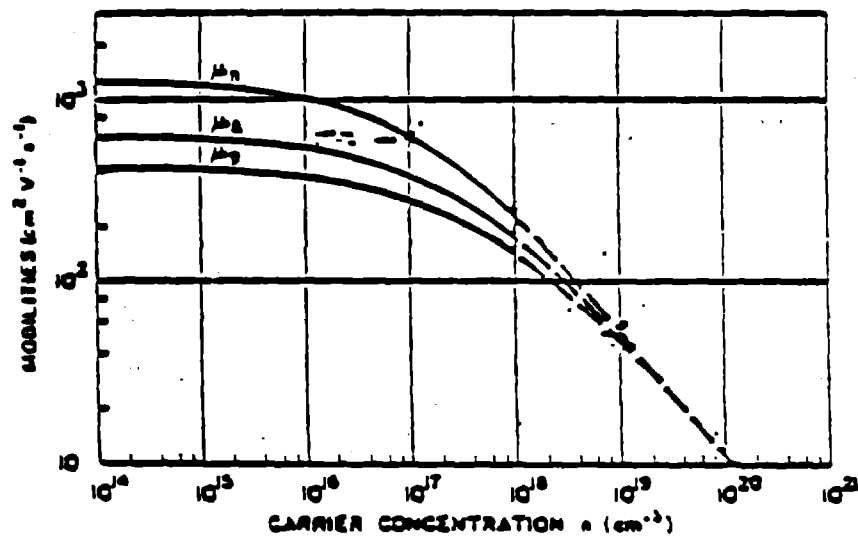
REFERENCES

- [1] G. Mourou and W. Knox, "High-Power Switching With Picosecond Precision," Appl. Phys. Lett. 35, October, 1979.
- [2] D. L. Scharfetter and H. K. Gummel, "Large Signal Analysis of a Silicon Read Diode Oscillator," IEEE Trans. Electron Devices, ED-16, 64, 1969.
- [3] C. Jacoboni, C. Canali, G. Ottaviani, and A. Quaranta, "A Review of Some Charge Transport Properties of Silicon," Solid State Electronics, 20, p. 77, 1977.
- [4] A. Blicher, "Field-Effect and Bipolar Power Transistor Physics," Academic Press, New York, 1981.



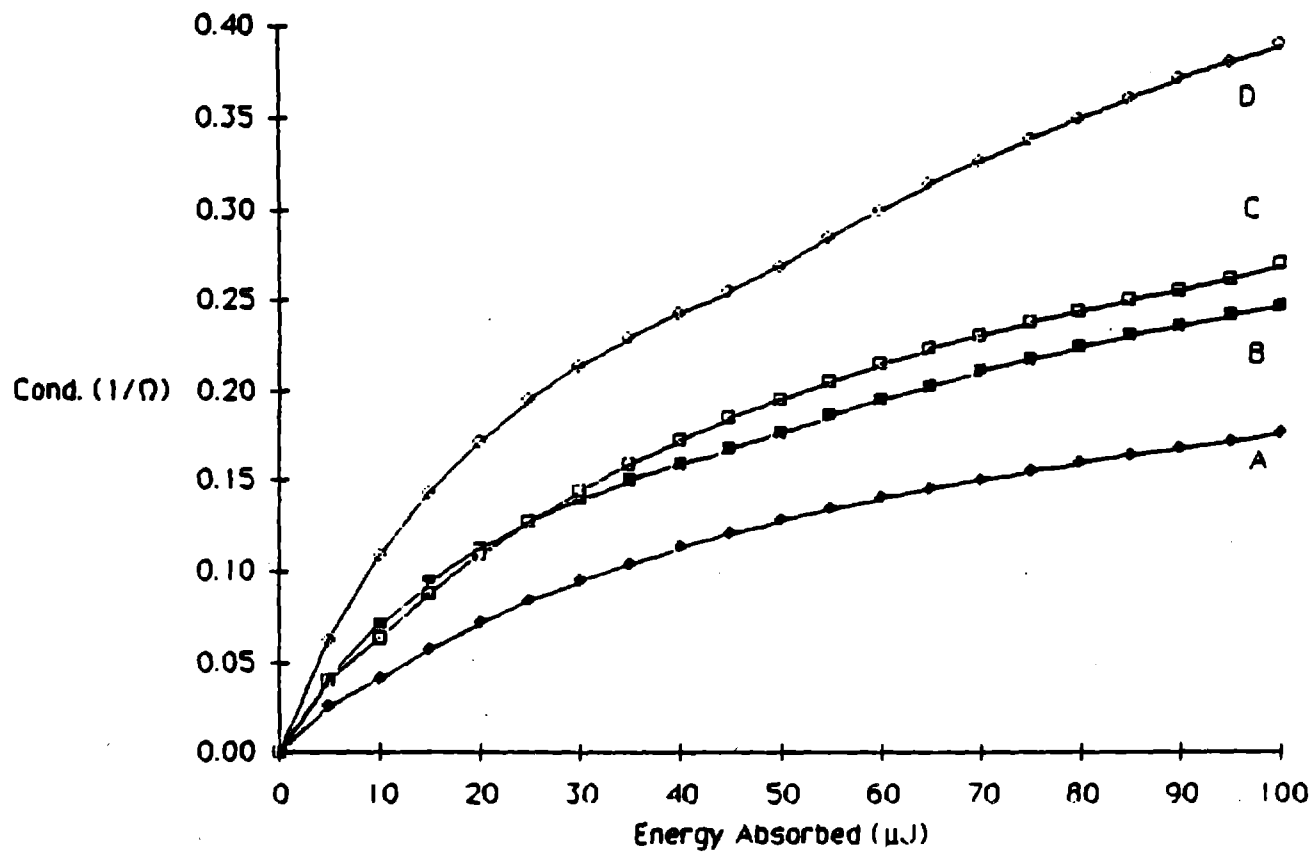
Silicon Photoconductive Switching Device Structure

FIGURE 1



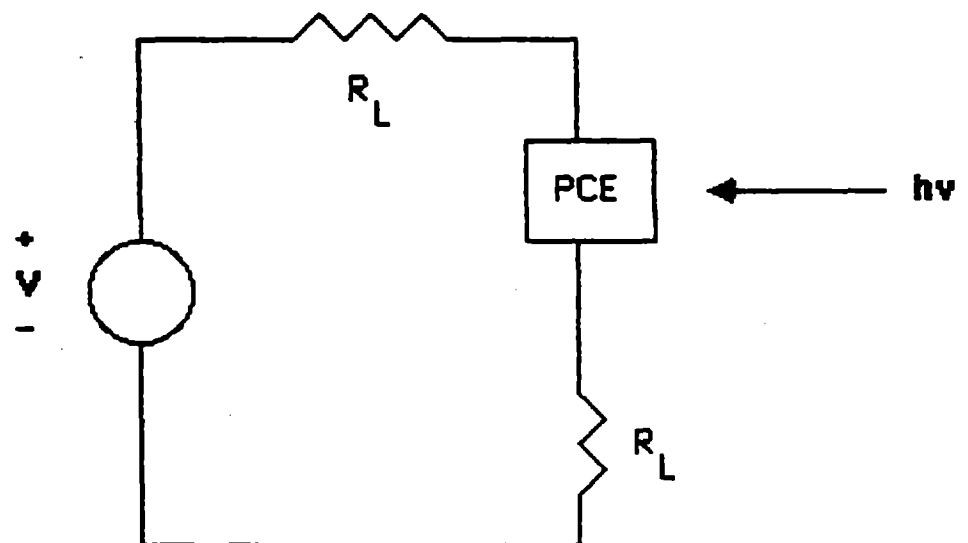
Electron (μ_n), hole (μ_p), and ambipolar (μ_a) mobilities as a function of a carrier concentration (From [4]).

FIGURE 2



Switch conductance as a function of absorbed energy assuming a carrier concentration dependent mobility.

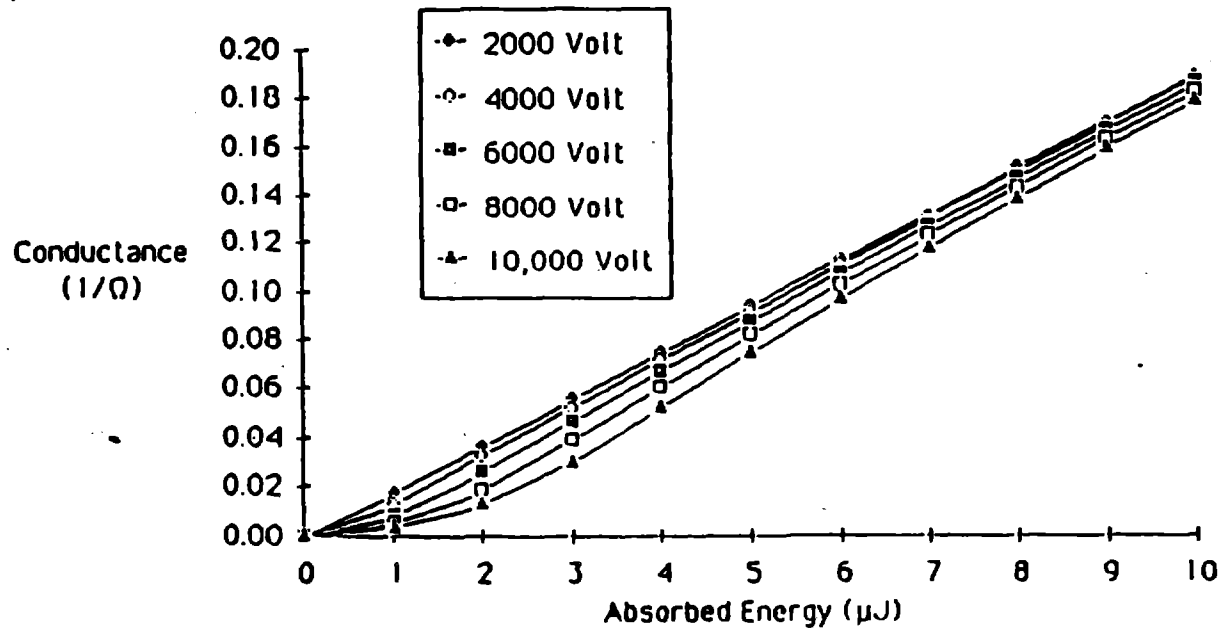
FIGURE 3



Equivalent circuit of photoconductive switch
mounted on 50 ohm transmission lines

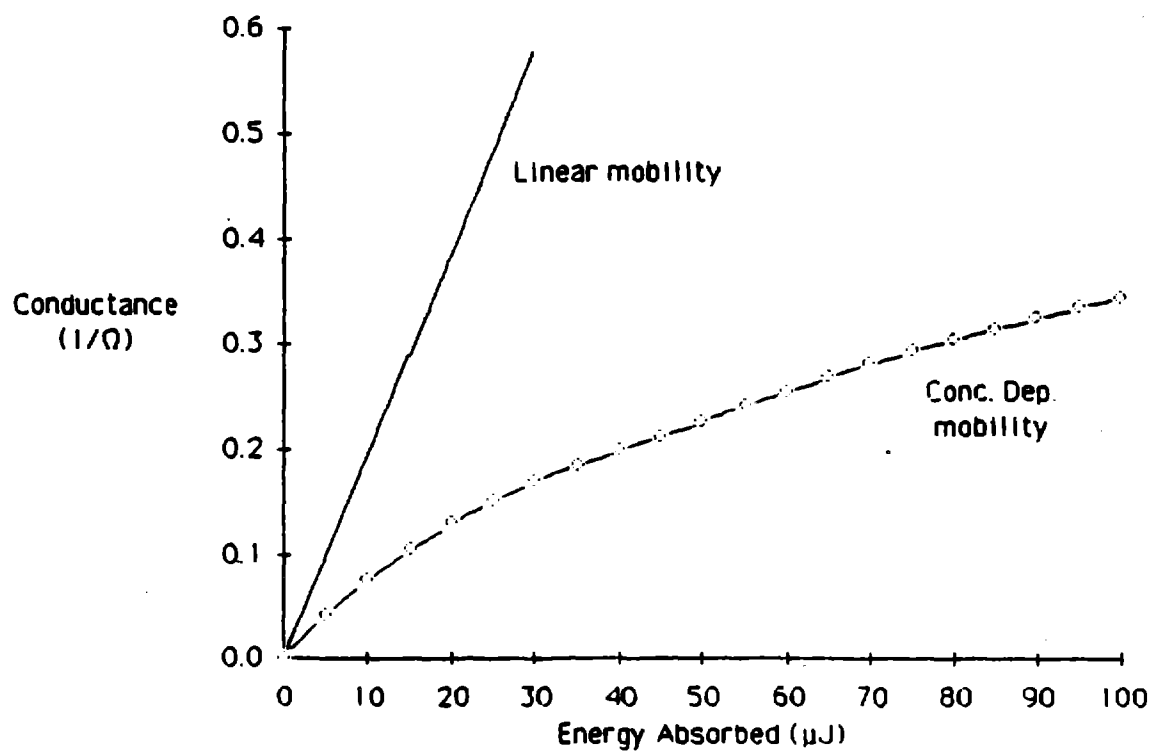
FIGURE 4

Photoconductive switch Light sensitivity



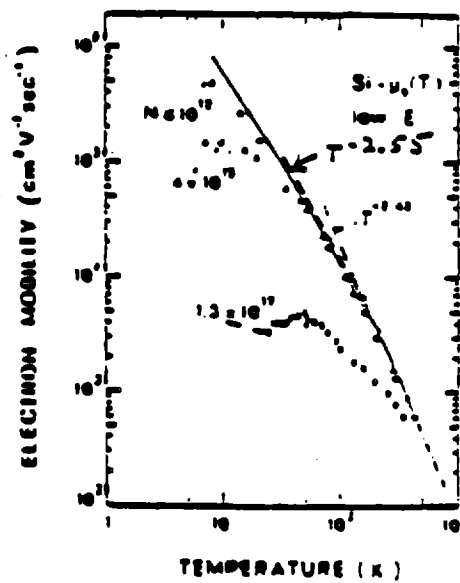
Switch conductance as a function of absorbed energy assuming field dependent mobility.

FIGURE 5

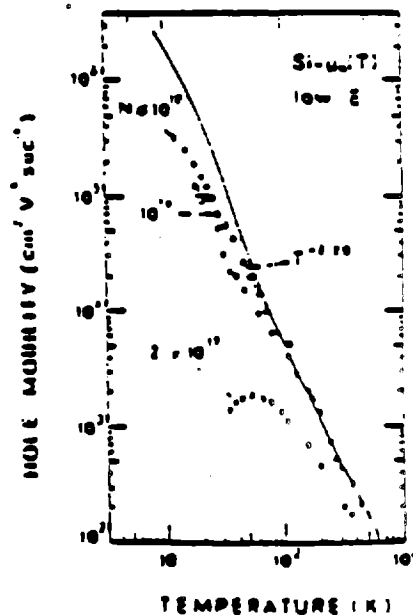


Comparison of switch conductance as a function of absorbed energy for constant mobility and electric field, carrier concentration dependent mobility.

FIGURE 6

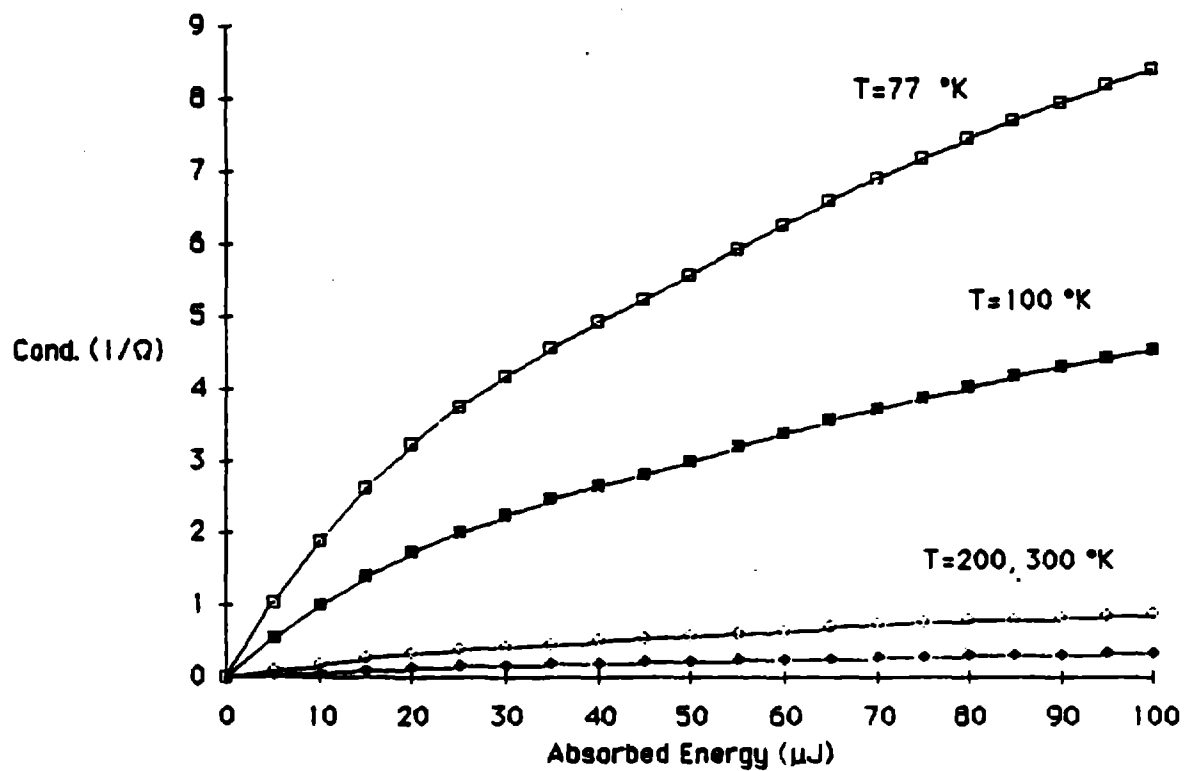


- a) Ohmic mobility of electrons in silicon as a function of temperature. It can be seen that for $T < 100^\circ\text{K}$, the electron mobility has a $T^{-2.55}$ dependence on temperature (from [3]).



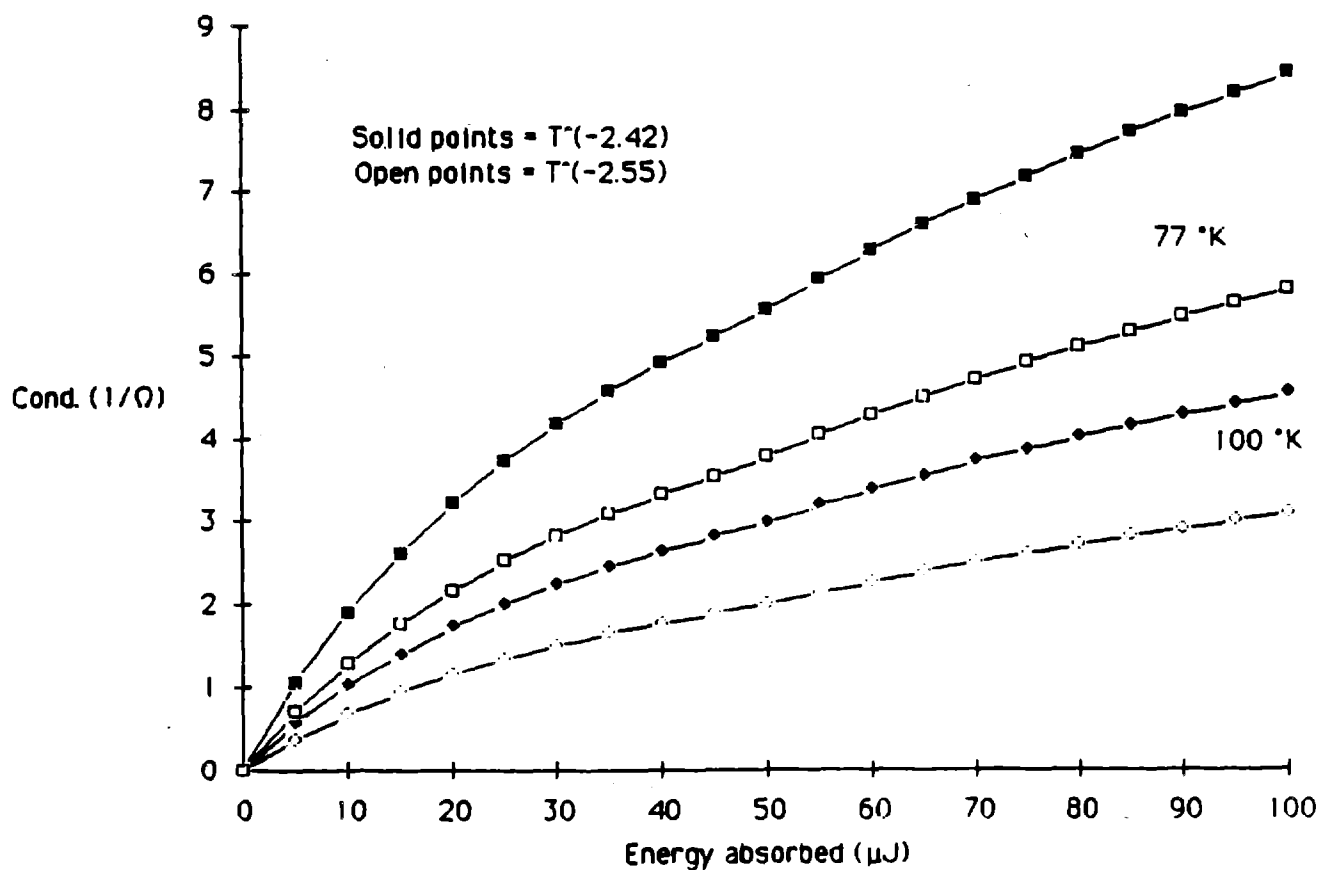
- b) Ohmic mobility of holes in silicon as a function of temperature. The solid line shows a $T^{-2.2}$ dependence of hole mobility on temperature (from [3]).

FIGURE 7



Switch conductance as a function of absorbed energy at T=77, 100, 200 and 300 °K.

FIGURE 8



Switch conductance as a function of absorbed energy
for $\mu_n \propto T^{-2.42}$ compared to $\mu_n \propto T^{-2.55}$

FIGURE 9